SUPPLEMENTARY TEXT

Cell culture, transfection and synchronization

U2OS, HeLa, T98G cells were grown in DMEM supplemented with 2 mM glutamine, 1 mM sodium pyruvate, 10 U/L penicillin, 10 μg/L streptomycin and 10% fetal bovine serum (Gibco). NIH3T3 cells were grown in the same conditions, but using 10% calf serum (ATCC). Sub-confluent U2OS cells were transfected using Effectene reagent (Qiagen), while confluent NIH3T3 cells with Lipofectamine 2000 (Invitrogen), following the manufacturer's protocol. Cells were usually imaged or processed for biochemistry 24-48h after transfection. U2OS cell lines stably expressing the desired recombinant fluorescent construct were generated by selecting transfected cells with 700 μg/ml Neomycin (Gibco); they were pooled and further cultured for 2-3 weeks in the constant presence of antibiotic. U2OS cells were synchronized at G1/S border by 24 hours incubation with 5μg/ml aphidicolin (Sigma). T98G cells were synchronized in G1 phase by incubating cells for 72 h in serum free DMEM and collecting them 5h after release in complete medium. To arrest T98G cells in late G1, G1/S border and S phases, they were treated with 0.5mM mimosine for 24h and collected directly, 2h and 6h after mimosine release, respectively. To arrest the cells in M phase cells were treated 17h with 2.5mM thymidine, released for 9h in complete medium and treated 17h with nocodazole 50ng/ml. The cells were stained with propidium iodide and cell cycle progression was followed by flow-cytometric analysis.

Expression constructs

RFP-PCNA (1) was a kind gift of M.C. Cardoso and H. Leonhardt. NLS_{SV40}-mCherry was cloned in the Kpn/BamHI sites of a pcDNA3.1 vector (Invitrogen) and used as control in FRAP experiments. mCherry was also cloned alone in the HindIII/BamHI sites of a pcDNA3.1/Hygro vector (Invitrogen) and used as control in FRET experiments. The cloning strategy of both full length HOXC13 (1-330) and that of the homeodomain deletion mutant (1-257) downstream a mCherry or EGFP fluorophore, has been previously described (2). Site-directed mutagenesis (Stratagene Site-directed Mutagenesis Kit) was performed to obtain the HBX-mutants from the wt mCherry-HOXC13 template. The cDNA of ORC2 and Cdc6 proteins were cloned into pEGFP-C1 vectors (Clontech). EGFP-MCM3 and ORC1-EGFP constructs were a kind gift of R. Paolinelli and R. Mendoza-Maldonado. All these EGFP constructs, together with the EGFP-NLS_{SV40} control, were subjected to EGFP-point mutation to generate E^0GFP fluorophore (3), chosen as donor in the FRET experiments.

FRAP acquisition and data analysis

All images were acquired using a 60X/1.42NA oil immersion objective, a frame size of 256×256 pixels (0.138 μm constant pixel size), 543nm laser power set between 10 and 20 μW and pinhole set to 200 μm (≈ 2AU) in order to increase the signal and to acquire a significant height of the nucleus. mCherry photobleaching was achieved using a single pulse with all 543, 514, 488, 458 laser lines set to full power for the necessary time to bleach a ROI covering half of the nucleus (typically: 250-600 msec, depending on the nucleus size). Time series were recorded for 5 minutes at 0.129 ms/frame sampling rate with 20 pre-bleach frames for slow proteins; for 30

seconds at 0.065ms/frame sampling rate with 5 pre-bleach frames for fast constructs (NLS_{SV40}-mCherry and HOXC13 deletion mutant). The average fluorescence intensities of the bleached area for each time point were background substracted, normalized to the pre-bleach average value and also for total nuclear fluorescence. Data were finally normalized for the bleach depth (4). For each analyzed construct the FRAP curves of 10-40 cells were averaged and the mean curves (±SE) are reported in the graphs of Figs. 2 and 3.

For FRAP data fitting, a reaction-diffusion model was used, which describes a situation where a molecule can diffuse freely or undergo a binding reaction with immobile sites, of the type:

$$F + S \underset{k_{on}}{\overset{k_{off}}{\rightleftarrows}} C, \qquad (1)$$

where F represents free molecules, S vacant binding sites, C bound [FS] complexes, and k_{on} and k_{off} are the on- and off-rates, respectively (5,6). In order to apply the model to the analysis of half-nuclear FRAP experiments, we assume that the biological system has reached equilibrium before photobleaching, and that the number of free binding sites [S] does not fluctuate appreciably during the FRAP experiment; under these assumptions, applicable in many biological situations, one can consider a pseudo-first-order rate constant given by $k_{on}^{*} = k_{on}[S]_{eq}$, where $[S]_{eq}$ is the concentration of the binding sites at equilibrium; we consider $[S]_{eq}$ homogeneous as a further simplification (6).

The reaction-diffusion model equations reduce therefore to the form:

$$\begin{aligned} \frac{\partial f}{\partial t} &= D\nabla^2 f - k_{on}^{*} f + k_{off} c \\ \frac{\partial c}{\partial t} &= k_{on}^{*} f - k_{off} c, \end{aligned} \qquad (2)$$

where $c=[C]$, $f=[F]$, and D is the diffusion coefficient for F. Boundary conditions require no flux of F cross the boundary; at equilibrium, $c=K f$, where $K = \frac{k_{on}^{*}}{k_{off}}$ (6). We substituted in (2) $k_{on}^{*} = K k_{off}$ and calculated, using Wolfram Mathematica 6.0.1.0, the solution of the Fourier-transform in $\vec{r}$ of the resulting system of differential equation with the initial condition $\tilde{c}(q,t=0) = K\tilde{f}(q,t=0) \equiv 1$ ($\vec{q}$ is the transform variable of $\vec{r}$ and the solutions depend only on $q = |\vec{q}|$).

The FRAP recovery curve for the "half-FRAP" geometry discussed in the main text can be approximated by the function:

$$h(t;D,K,k_{off}) = 1 + \frac{4}{l\left(1+K^{-1}\right)} \sum_{n=1}^{N} \frac{-2l}{(2n+1)^2 \pi^2} \left[\tilde{f}\left(\frac{(2n+1)\pi}{l}, t \right) + \tilde{c}\left(\frac{(2n+1)\pi}{l}, t \right) \right], \qquad (3)$$

where the dependence on the parameters D, K and k_{off} in every term on the right is not explicit, N is the number of non-zero terms considered in the Fourier series, and l is the total length of the rectangular parallelepiped best approximating the nucleus.

Equation (3) derives from the Fourier series for the 1D solution of (2), or better for the solution for a nucleus approximated as a rectangular parallelepiped, with initial conditions that the border

between the bleached and unbleached parts is a symmetry plane of the system. $h(t)$ is the integral of $c(\vec{r},t)+f(\vec{r},t)$ in the bleached part, and represents the change of the average fluorescence in the bleached part normalized between 0 (at the starting time) and 1 (after total recovery).
Since the bleach depth normalization in the experimental FRAP data forces them to start at zero, in order to correct for truncation or rounding errors we fitted the data with the function

$$\frac{h(t;D,K,k_{off})-h(0)}{1-h(0)}, \qquad (4)$$

where $h(t=0)$ is usually <<1 in absolute value, does not depend on the values of D, K and k_{off}, but depends on N.
We verified that the results of the fit didn't change significantly for N between 6 and 15; for the results presented in this work, N was usually 10 (actually corresponding to a Fourier series with 22 terms, including the first one for $q=0$). We checked in selected cases that there was a clear minimum for the χ^2 (proportional to the sum of the square of the residuals from fit); this was clearly the case considering the plane of parameters (D, k_{off}) and (K, k_{off}), whereas this analysis revealed a strong correlation in the plane (D, K), with the consequence that a bigger uncertainty is expected for these parameters.
In the main text, instead of K, we reported the fraction of free protein:

$$F_{free} = \frac{[F]_q}{[F]_q + [C]_q} = \frac{1}{1+K};$$

moreover, we indicated D as D_{app} since it could include, besides free nucleoplasmic diffusion, the possibility of unspecific/transient chromatin interaction by the protein (5). The fit applied to the FRAP curves of all 40 analyzed cells, expressing transiently wt mCherry-HOXC13, led to the following results: D_{app}= 5.10±3.88μm^2/s, F_{free}=42.0±24.7%, K_{off}=0.008± 0.003s^{-1}. Results reported in Fig. 2D actually refer to a selection of the 16 cells which best fitted the model geometry; in detail, nuclei which moved significantly vs. the bleached or unbleached region during the time series, nuclei in which the bleached region was in length less than 44% of the whole nucleus, nuclei presenting a visible non-homogeneity between bleached and unbleached regions, were discarded.

Antibodies

The following antibodies were used: rabbit polyclonal α-HOXC13 (2) and rabbit polyclonal α-HOXC10 produced and purified by immunization of rabbit with GST-tagged HOXC10 (1-231) lacking the conserved homeodomain; mouse monoclonal α-tubulin (clone B-512, Sigma), mouse monoclonal α-actin (clone AC-40, Sigma or clone C-4, Santa Cruz Biotechnology), goat polyclonal α-ORC2 (clone B-18, Santa Cruz Biotechnology), rabbit polyclonal and mouse monoclonal α-GFP (ab290, ab12518 Abcam), mouse monoclonal α-Cdc6 (clone D-1, Santa Cruz Biotechnology), rabbit polyclonal α-Cdc6 (clone H-304, Santa Cruz Biotechnology), rabbit polyclonal α-USF1 (clone C-20, Santa Cruz Biotechnology). BrdUrd immunofluorescence was previously described (2).

Cell fractionation

Typically, 3-5×10^7 cells were used for each fractionation. Cells were harvested by trypsinization, counted and washed twice with ice-cold PBS. 5×10^6 cells were lysed in RIPA buffer (Sigma) and

further referred to as whole cell extract. The remaining cells were sequentially fractionated. First cytoplasm was extracted, similarly to what already reported (7,8), resuspending cells (at 4×10^7cells/ml) in ice-cold 15mM Tris-HCl pH 7.5, 10mM KCl, 10mM NaCl, 5mM $MgCl_2$, 1mM $CaCl_2$, 300mM sucrose, 10% glycerol and 0.1% Triton-X100 for 7'. Low-speed centrifugation (1300g, 5') allowed separating cytoplasm (supernatant) from intact nuclei. These were washed three times before performing the nucleoplasm extraction (at 1.2×10^8cells/ml) in ice cold 25mM Tris-HCl pH 8, 20mM NaCl, 5mM $MgCl_2$, 1mM EDTA, 10% glycerol and 0.5% NP-40 for 20'. Low-speed centrifugation (1500g, 5') allowed separating nucleoplasm (supernatant) from chromatin. Chromatin was washed once and then salt-extracted in ice-cold 25mM Tris-HCl pH 8, 0.5mM $MgCl_2$, 300mM sucrose, 10% glycerol and sequentially increasing NaCl concentrations (150, 300, 600, 2M NaCl). The 150mM extraction step was either performed without or with 200U DNase I (Roche) and 6mM $MgCl_2$ (in this case at 22°C). Each extraction step lasted 30' under rotation and was followed by centrifugation at 14000g for 5' before subsequent pellet extraction with increasing NaCl. All obtained fractions were clarified (at 16000g for 30'). The described buffers were supplemented with protease inhibitors (leupeptin, aprotinin, PMSF), phosphatase inhibitors (NaF, Sodium orthovanadate), 1mM DTT and 1mM ATP prior to use. Protein concentration was estimated by Bradford assay (Pierce) and ~30µg were used for the detection of each fraction by Western Blot.

GST pull-down assay

Bacterial cultures were grown in culture broth + ampicillin and protein production was induced with IPTG 1 mM for 4 hours at 30°C with OD600 between 0.6 and 0.8. Bacteria were then resupended in cold lysis buffer (50 mM Tris-HCl pH 8, 5 mM EDTA pH 8, 250 mM NaCl, 5% glycerol, proteases inhibitor) and sonicated. Bacterial lysates were mixed with a 50% slurry of glutathione cross-linked agarose beads and the GST-fusion proteins were allowed to bind the beads at 4°C on a rotating wheel for 1 hour. The suspension was then loaded on an empty plastic column, letting the unbound proteins pass through, and the beads were washed with lysis buffer. The purity and integrity of the proteins were routinely checked by SDS-PAGE and Coomassie blue staining. To remove contaminant bacterial nucleic acids, recombinant proteins were pretreated with nucleases (0.25 unit/µl DNase I and 0.2 µg/µl RNase) for 1 hr at 25°C in 50 mM Tris-HCl, pH 8/5 mM $MgCl_2$/2.5 mM $CaCl_2$/100 mM NaCl/5% glycerol/1 mM DTT. Then the GST fusion proteins immobilized on agarose beads were washed and resuspended in NETN buffer (20 mM Tris-HCl, pH 7.5/100 mM NaCl/1 mM EDTA/0.5% Nonidet P-40/1 mM DTT/1 mM phenylmethylsulfonyl fluoride) supplemented with 0.1 mg/ml ethidium bromide to impede the possible formation of nonspecific interactions between residual DNA and proteins. [^{35}S]-labelled proteins was added and incubated at 4°C on a rotating wheel. After 1hr, bound proteins were washed five times with 1 ml of NETN buffer and separated by electrophoresis in an SDS/7% polyacrylamide gel. Dried gels were quantitated by phosphoimaging (Cyclone).

ChIP and co-immuno-precipitation

Chromatin immuno-precipitation (ChIP) was done as previously described (2). ChIP on HOXC10 was done using native-ChIP HAP protocol (9) with some differences: nuclei were isolated from cultured T98G cells, chromatin was fragmented to mononucleosomal size using MNase, chromatin was purified using HAP, the eluate was then dialyzed to a buffer suitable for IP

(25mM Tris-HCl pH 8.0, 150mM NaCl, 1mM EDTA, 0.05% SDS, 0.1% NP40); HOXC10 was immuno-precipitated using Millipore Upstate ChIP Assay kit and its protocol; immuno-precipitated DNA was analyzed by competitive PCR (10). For the co-IP, total extract was prepared from asynchronous T98G cells as previously described in the ChIP experiment of HOXC13. The lysate was incubated with protein A on agarose beads for 1h. The supernatant was collected and incubated over night with rabbit polyclonal α-Cdc6 antibody, with polycolonal antibody α-USF1 and rabbit α-IgG as negative control. The immunocomplexes were collected with protein A on agarose beads and washed with buffers from Chromatin Immuno-precipitation (ChIP) Assay Kit (Millipore) supplemented with 1mM PMSF and protease inhibitors cocktail tablet (Roche). The immuno-precipitated material was divided for separately western blotting analysis with mouse antibody α-Cdc6 and rabbit antibody α-HOXC13. The co-immuno-precipitation of endogenous ORC2 and GFP-HOXC13 was performed using a combination of DNase I + 600 mM NaCl nuclear extract of U2OS cells transfected with EGFP-HOXC13. 250 μg of nuclear extract (1:10 diluted in PBS) were incubated for 2h at 4°C with Dynabeads-protein A (Invitrogen), previously functionalized either with rabbit α-GFP, or with control rabbit IgG. Beads were washed twice with a 300 mM NaCl phosphate buffer before investigation of the immuno-precipitated proteins by Western Blot.

FLIM acquisition and data analysis

Measurements were performed with a Leica TCS SP2 inverted confocal microscope (Leica Microsystems), interfaced with fast photon counting external detectors (Hamamatsu, H7422P-40) and time-correlated single-photon counting (TCSPC) electronics (Becker & Hickl). The system was equipped with a heated chamber set to 37°C and 5% CO_2. All images were acquired using a 40X (NA 1.25) oil immersion objective. First, reference intensity images were obtained for E^0GFP constructs and, when co-expressed, mCherry constructs, at 512×512 frame size using 488 and 561 nm laser lines, respectively. Then the donor image was acquired at 128×128 frame size using the photon counting mode: in this case 403nm-excitation of E^0GFP was achieved using a pulsed diode laser (M8903-01; Hamamatsu) set at 10MHz repetition rate and 3-5 μW laser power. These conditions ensured neither photobleaching nor photoactivation of the donor fluorophore, as well as photon counting rates between 10^4–10^5 cps. Time of acquisition ranged from 80 to 200s (typically 120s), depending on donor expression level. These images were used to obtain lifetime values from fluorescence decays using a pixel-by-pixel fitting procedure. Usually fluorescence decays were optimally fitted after binning of 1-3. Only pixels within cell nuclei were considered: lifetimes were repeatedly fitted until all nuclear pixels displayed a $\chi^2 \leq 1.3$. First, decays of cells expressing donor alone were fitted with a monoexponential decay equation, to obtain the mean lifetime value of the donor alone, τ_D. When the donor was expressed with the acceptor, it was assumed to exist either in the unbound or in the acceptor-bound state; therefore data were fitted with the following biexponential equation:

$$I(t) = a_1 \cdot e^{-\frac{t}{\tau_{DA}}} + a_2 \cdot e^{-\frac{t}{\tau_D}}$$

where τ_D was known from the previous monoexponential fit and therefore was fixed. τ_{DA}, the shorter lifetime of the donor involved in FRET with the acceptor, was the fitting parameter together with a_1 and a_2. The resulting τ was an average of τ_D and τ_{DA} components weighted for the respective subpopulations. In the Results session, both τ derived from mono- and bi-exponential fittings are referred to as τ_m (mean lifetime). Lifetime distribution histograms were

obtained from all analyzed nuclei and were normalized to the nucleus area (i.e. pixels number). The sum of all distribution histograms of each sample was used to calculate the weighted mean lifetime, τ_m, reported in Table I. This sum histogram was also fitted with a standard Gaussian curve for presentation purposes (see graphs of Fig. 7). The peak value of the Gaussian curves is representative of the τ_m reported in Table I; moreover these graphs give an idea of the distribution of lifetime values around τ_m. The fitting analysis was performed with SPC-Image software (Becker & Hickl). Data and images were further analyzed by Origin Pro 7.0 and ImageJ softwares.

RNA depletion and stable clones production

T98G and U2OS cells were transiently transfected for 24h, 48h and 72h with lentiviral pGIPZ shRNA vector (Open Biosystems) encoding a short hairpin RNA against HOXC13 (NM_017410) within a region spanning nt 1186-1207 by Polyfect tranfection reagent (Qiagen) following the manufacturer's instructions. RNA interference control experiments were performed using an empty lentiviral pGIPZ vector (Open Biosystems). The HOXC13 downregulated clone and the control clone were selected using puromycin (3 μg/ml) after 48h of transient transfection followed by 12 days of selection.

BrdUrd incorporation

Synchronized cells were pulsed for one hour at a final concentration of 45μm and collected directly or 4h after release from mimosine or aphidicolin. BrdUrd detection was done by a primary antibody (Abcam) subsequently detected using a secondary antibody conjugated to AlexaFluor488. Cells were stained with propidium iodide and analyzed by double flow-cytometry analysis by FACSCalibur (Becton-Dickinson) instrument.

Nascent DNA preparation

HeLa cells were collected by scraping, resuspended in PBS containing 10% glycerol and lysed for 10 minutes in the wells of a 1.2% alkaline agarose gel immersed in alkaline running buffer: 50mM NaOH, 1mM EDTA. The gel was run for 16 hours at 2V/cm and the nascent DNA of size 0.6-1 kb was isolated from the gel using a Qiagen Gel Extraction kit. The isolated nascent DNA was analyzed by competitive PCR. The quantification of the abundance of the origin (B48) and non-origin (B13) DNA fragments was performed as described previously (10).

SUPPLEMENTARY FIGURES

Figure S1

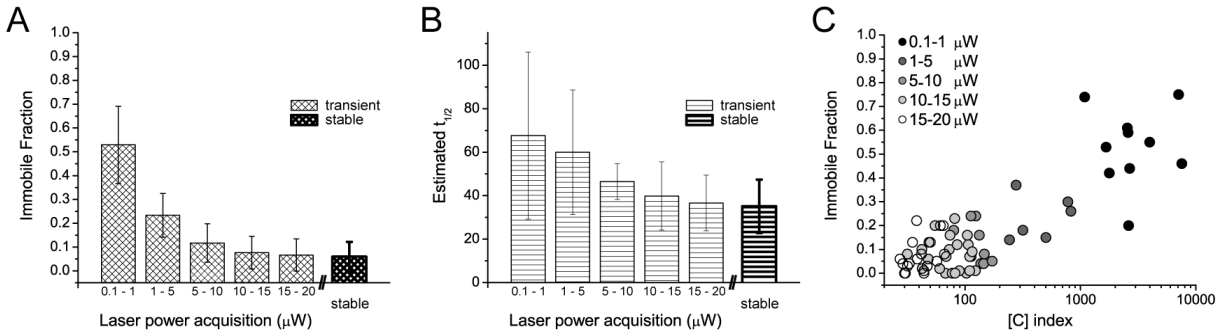

Figure S2

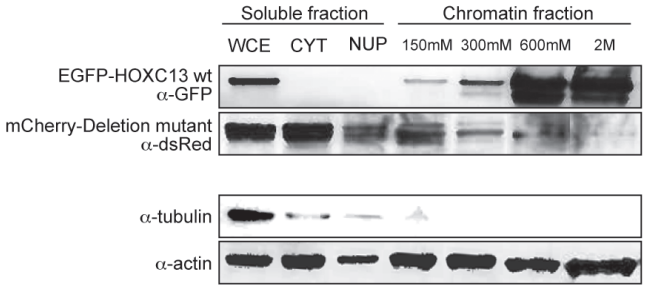

Figure S3

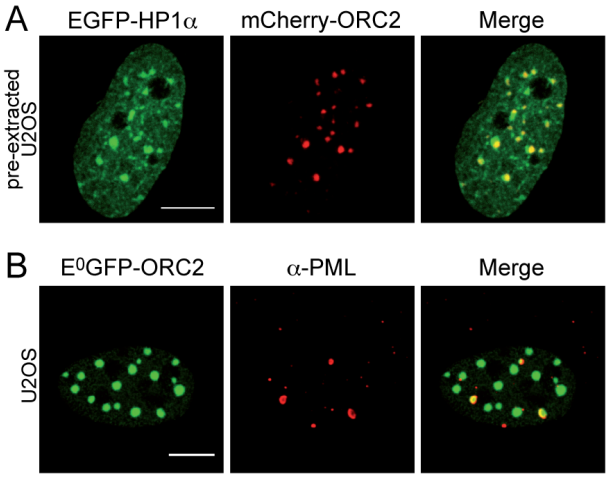

Figure S4

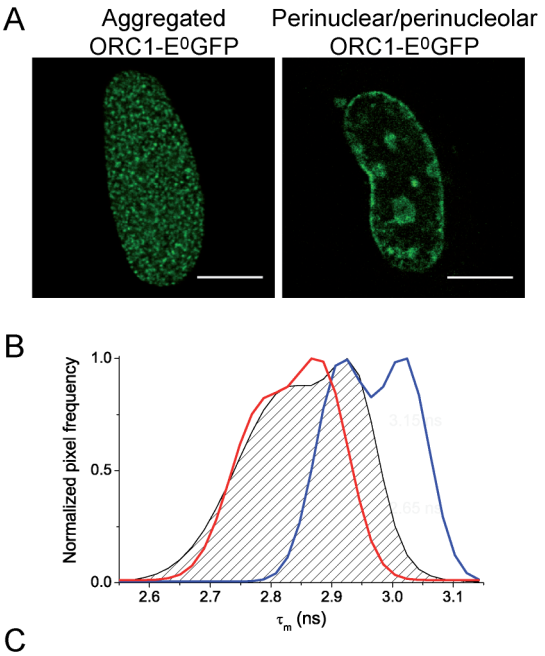

C

Sample	τ_m	n
ORC1-E⁰GFP alone	2.96±0.05 ns	62
ORC1-E⁰GFP + mCherry	2.84±0.05 ns	48
ORC1-E⁰GFP + mCherryHOXC13	2.83±0.04 ns	72

Figure S5

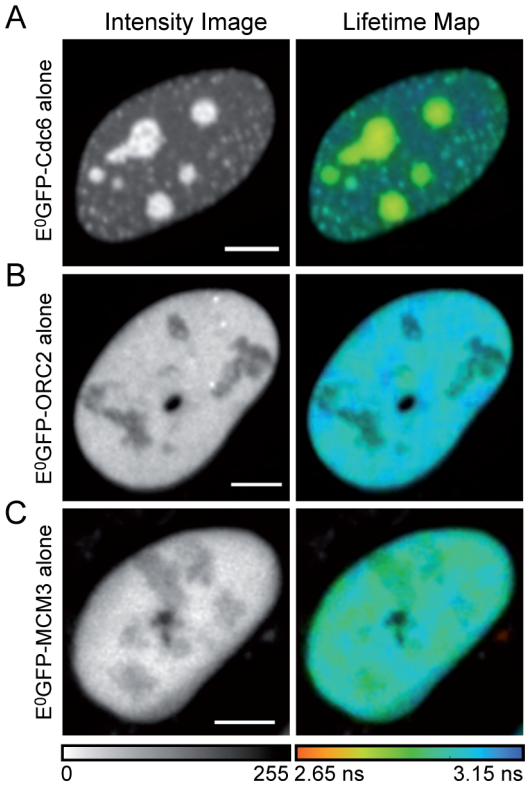

Figure S6

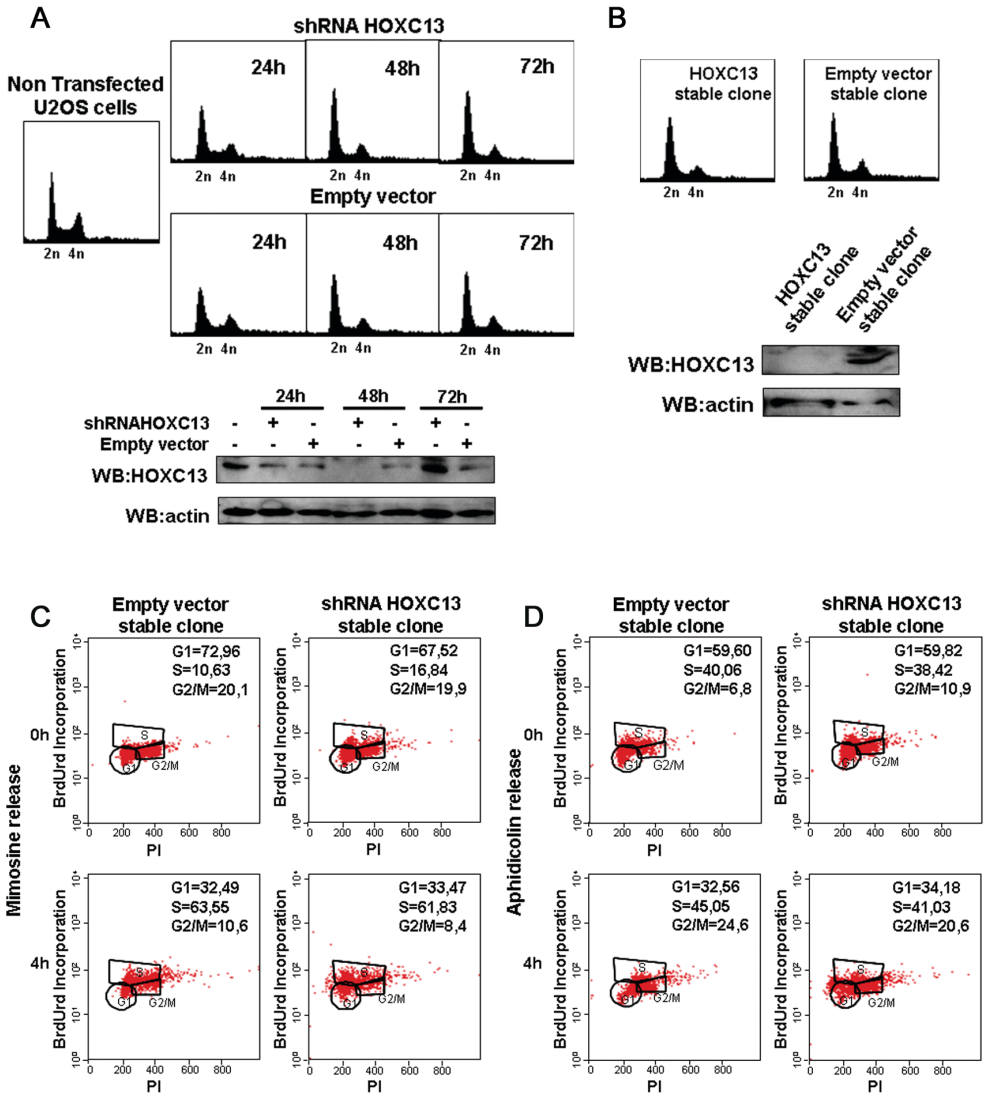

SUPPLEMENTARY FIGURE LEGENDS

Figure S1. Dependence of wt mCherry-HOXC13 nuclear dynamics on expression levels. To study the dependence of HOXC13 nuclear dynamics on protein expression levels, FRAP measurements were performed using the same set up parameters, with the exception of acquisition laser power. In this way, laser power was directly linked to the expression level (high expression levels need low laser power to be visualized, vice versa for low expression levels). FRAP curves were measured for cells (n=67) presenting different protein expression levels, and $t_{1/2}$ and immobile fraction were estimated from the recovery curve of each of them. Mean estimated $t_{1/2}$ (panel **A**) and immobile fraction (panel **B**) of all analyzed cells plotted vs. laser

power ranges of acquisition (from 0.1-1 to 15-20 μW) reveal a clear dependence of the two parameters on the protein expression levels (error bars are SD). Precisely, very high protein concentration values (0.1-1 μW) lead to very high and uncertain $t_{1/2}$ and immobile fraction values. Instead, as protein concentration decreases (10-20 μW), both $t_{1/2}$ and immobile fraction reach stable values comparable to those obtained for a stable expression of the construct (bold histogram bars). Therefore only cells with low expression profile (10-20 μW laser power acquisition range) were used to obtain the mean FRAP curve reported in Fig. 2C. (**C**) Dependence of the immobile fraction on protein concentration, expressed as [C] index: this was calculated as a ratio between mean pre-bleach nuclear fluorescence and acquisition laser power. Different gray-scale tones correspond to different laser power ranges of acquisition.

Figure S2. Biochemical fractionation of U2OS cells expressing fluorolabelled constructs of wt HOXC13 (first row from the top) and Deletion mutant (second row from the top). The soluble (left) and chromatin (right) fractions were investigated for the presence of GFP-HOXC13 and mCherry-Deletion mutant by Western Blot (tubulin and actin are loading controls). All fractions were compared to the protein level detected in a whole-cell extract (WCE). CYT and NUP are cytoplasmic and nucleoplasmic fractions, respectively. The chromatin fractions are identified by the NaCl concentration used for the extraction.

Figure S3. Heterochromatic nature of E^0GFP-ORC2 nuclear aggregation. As reported for endogenous ORC2 protein (11-13), the E^0GFP-ORC2 focal structure displayed in G1 phase (Fig. 6B), relies on the association with heterochromatin. (**A**) GFP-HP1a and mCherry-ORC2 co-localize in the same foci (see the Merge image) in U2OS cells subjected to 0.5% TritonX-100 pre-extraction prior to fixation (2). (**B**) E^0GFP-ORC2 foci partially co-localize with PML bodies (immunostained with a-PG-M3 antibody, Santa Cruz Biotechnolgy, and detected with an Alexa-647 conjugated secondary antibody), which also take part to the heterochromatin structure (14). Scale bar: 5 μm.

Figure S4. FLIM measurements were performed to probe the interaction between mCherry-HOXC13 and ORC1-E^0GFP. (**A**) Two different nuclear localizations were observed for ORC1-E^0GFP construct, one displaying densely spotted ORC1 throughout the nucleus (left), and the other one reporting ORC1 on nuclear periphery and in nucleoli (right). No clear cell-cycle dependence of the two localizations was found by 20-24h time-lapse imaging (data not shown). Both ORC1 distributions were tested for the interaction with HOXC13. Scale bar: 10 μm. (**B**) FLIM analysis of an equal amount of the two ORC1 phenotypes resulted in a double peaked lifetime distribution for the donor alone (blue curve) as well as for the donor with acceptor (the dashed area represents the negative control performed expressing ORC1-E^0GFP with untagged mCherry; the red curve is the co-expression of ORC1-E^0GFP with mCherry-HOXC13). In all three curves, the peaks at lower lifetime correspond to the more aggregated ORC1 phenotype (left image of panel **A**). (**C**) Table summarizing the final lifetime values obtained in this FLIM study (mean±SE): no significant difference between the negative control and the ORC1-HOXC13 sample could be detected *in vivo*. It is possible that the aggregated ORC1 phenotype can lead per se to a lower lifetime with respect to the other perinuclear, less concentrated, ORC1 phenotype. This artifact could also be responsible of the 2-fold increased unspecific FRET signal detected for the negative control of ORC1-E^0GFP, when compared to the other probed proteins

(Table I). It must be underlined that this wide range of unspecific interaction compromises any further consideration on the lifetime distribution curve obtained for ORC1 in the presence of HOXC13.

Figure S5. Fluorescence lifetime maps of E^0GFP-RC proteins expressed alone in U2OS cells. Fluorescence intensity images (left) and corresponding lifetime maps (right) of E^0GFP fused to Cdc6 (**A**), ORC2 (**B**), MCM3 (**C**) proteins expressed alone in U2OS cells. Each lifetime map is superimposed on the corresponding intensity image. All three lifetime maps share a common blue-shifted color, corresponding to donor lifetime values ~ 3 ns, similarly to what reported for untagged E^0GFP (15). Scale bar: 5 μm.

Figure S6. Down regulation of HOXC13. (**A**) Flow cytometry profiles of U2OS cells before and after transient transfection with lentiviral vector expressing anti-HOXC13 shRNA or with empty lentiviral vector. The cells were harvested and stained with propidium iodide 24h, 48h and 72h after the transfection and no significant modification in the profiles was detectable. Western blot analysis shows a nearly complete depletion of HOXC13 48h after the transfection with lentiviral vector expressing anti-HOXC13 shRNA. (**B**) Flow cytometry profiles of U2OS stably transfected with anti-HOXC13 shRNA or empty vector. The stably depletion of HOXC13 was detected by Wester blot. Actin was used as a blot control in both analyses. (**C**) Flow cytometry profiles of synchronized U2OS clones stably expressing either empty vector (left) or shRNA against HOXC13 (right). The cells were collected directly after the release from mimosine (0h) and 4h after the release. The cells were pulsed with BrdUrd and stained with an anti-BrdUrd antibody and analysed by flow citometry after Propidium Iodide staining. The gated cell population in the different phases of the cell cycle and the percentage of cells in each gate are indicated. (**D**) Same as in (**C**) but with collection of the cells after aphidicolin treatment.

SUPPLEMENTARY REFERENCES

1. Sporbert, A., Domaing, P., Leonhardt, H. and Cardoso, M.C. (2005) PCNA acts as a stationary loading platform for transiently interacting Okazaki fragment maturation proteins. *Nucleic Acids Res*, **33**, 3521-3528.
2. Comelli, L., Marchetti, L., Arosio, D., Riva, S., Abdurashidova, G., Beltram, F. and Falaschi, A. (2009) The homeotic protein HOXC13 is a member of human DNA replication complexes. *Cell Cycle*, **8**, 454-459.
3. Arosio, D., Garau, G., Ricci, F., Marchetti, L., Bizzarri, R., Nifosi, R. and Beltram, F. (2007) Spectroscopic and structural study of proton and halide ion cooperative binding to gfp. *Biophys J*, **93**, 232-244.
4. Xouri, G., Squire, A., Dimaki, M., Geverts, B., Verveer, P.J., Taraviras, S., Nishitani, H., Houtsmuller, A.B., Bastiaens, P.I. and Lygerou, Z. (2007) Cdt1 associates dynamically with chromatin throughout G1 and recruits Geminin onto chromatin. *Embo J*, **26**, 1303-1314.
5. Beaudouin, J., Mora-Bermudez, F., Klee, T., Daigle, N. and Ellenberg, J. (2006) Dissecting the contribution of diffusion and interactions to the mobility of nuclear proteins. *Biophys J*, **90**, 1878-1894.

6. Sprague, B.L., Pego, R.L., Stavreva, D.A. and McNally, J.G. (2004) Analysis of binding reactions by fluorescence recovery after photobleaching. *Biophys J*, **86**, 3473-3495.
7. Nielsen, A.L., Ortiz, J.A., You, J., Oulad-Abdelghani, M., Khechumian, R., Gansmuller, A., Chambon, P. and Losson, R. (1999) Interaction with members of the heterochromatin protein 1 (HP1) family and histone deacetylation are differentially involved in transcriptional silencing by members of the TIF1 family. *Embo J*, **18**, 6385-6395.
8. Mendez, J. and Stillman, B. (2000) Chromatin association of human origin recognition complex, cdc6, and minichromosome maintenance proteins during the cell cycle: assembly of prereplication complexes in late mitosis. *Mol Cell Biol*, **20**, 8602-8612.
9. Brand M, R.S., Chandra-Prakash C, Dilworth FJ. (2008) Analysis of epigenetic modifications of chromatin at specific gene loci by native chromatin immunoprecipitation of nucleosomes isolated using hydroxyapatite chromatography. *Nat. Protoc.*, **3**, 398-409.
10. Diviacco, S., Norio, P., Zentilin, L., Menzo, S., Clementi, M., Biamonti, G., Riva, S., Falaschi, A. and Giacca, M. (1992) A novel procedure for quantitative polymerase chain reaction by coamplification of competitive templates. *Gene*, **122**, 313-320.
11. Prasanth, S.G., Prasanth, K.V., Siddiqui, K., Spector, D.L. and Stillman, B. (2004) Human Orc2 localizes to centrosomes, centromeres and heterochromatin during chromosome inheritance. *Embo J*, **23**, 2651-2663.
12. Craig, J.M., Earle, E., Canham, P., Wong, L.H., Anderson, M. and Choo, K.H. (2003) Analysis of mammalian proteins involved in chromatin modification reveals new metaphase centromeric proteins and distinct chromosomal distribution patterns. *Hum Mol Genet*, **12**, 3109-3121.
13. Auth, T., Kunkel, E. and Grummt, F. (2006) Interaction between HP1alpha and replication proteins in mammalian cells. *Exp Cell Res*, **312**, 3349-3359.
14. Hayakawa, T., Haraguchi, T., Masumoto, H. and Hiraoka, Y. (2003) Cell cycle behavior of human HP1 subtypes: distinct molecular domains of HP1 are required for their centromeric localization during interphase and metaphase. *J Cell Sci*, **116**, 3327-3338.
15. Albertazzi, L., Arosio, D., Marchetti, L., Ricci, F. and Beltram, F. (2009) Quantitative FRET Analysis With the EGFP-mCherry Fluorescent Protein Pair. *Photochem Photobiol*, **85**, 287-297.